Ultrathin Seed−Layer for Tuning Density of ZnO Nanowire Arrays and Their Field Emission Characteristics

ARTICLE *in* THE JOURNAL OF PHYSICAL CHEMISTRY C · JULY 2008

Impact Factor: 4.77 · DOI: 10.1021/jp8015563

5 AUTHORS, INCLUDING:

Jun Chen
Sun Yat-Sen University
249 PUBLICATIONS **2,846** CITATIONS

SEE PROFILE

Ultrathin Seed-Layer for Tuning Density of ZnO Nanowire Arrays and Their Field Emission Characteristics

Jun Liu, Juncong She,* Shaozhi Deng, Jun Chen, and Ningsheng Xu*

State Key Laboratory of Optoelectronic Materials and Technologies, and Guangdong Province Key Laboratory of Display Materials and Technologies, School of Physics and Engineering, Sun Yat-Sen (Zhongshan) University, Guangzhou 510275, People's Republic of China

Received: February 21, 2008; Revised Manuscript Received: April 28, 2008

We report on how to tune the density of zinc oxide (ZnO) nanowire arrays in a wide range (more than 5 orders of magnitude) in a low temperature (80 °C) solution-phase growth process. A model based on the coexistence of nanowire growth and etching of the ultrathin (<3.5 nm) ZnO seed-layer was proposed to explain the effect. It was demonstrated that when the seed-layer thickness changes from 1.5 to 3.5 nm, the nanowire density increases from 6.8×10^4 to 2.6×10^{10} cm^{-2}. This significant variation of density with the seed-layer thickness was found to happen only when the layer thickness is within a few nanometers. If it is too thick (>3.5 nm), the variation is very narrow, and if it is too thin (<1.5 nm), no nanowires can grow. In addition, the density variation was accompanied by the change of both diameter and height of the nanowires, which leads to a change in aspect ratio. Both changes in density and aspect ratio were found to obviously affect the field emission characteristics. It was demonstrated that optimal conditions can be found to grow ZnO nanowire films with better field emission characteristics.

1. Introduction

Field electron emission from zinc oxide (ZnO) nanowires has attracted much attention in recent years due to their potential application in vacuum micro/nano electronic devices.[1–3] For obtaining good field emission performance from a nanowire film, it is important to find an optimal density of nanowires. Typically, high-density emission sites may be obtained while the field screen effect on the nanowire film is minimized. On the other hand, to have electron emission at low field, nanowires having a large aspect ratio are also desirable.[4] This requires one to make tall and thin nanowires. Investigation into how to find an optimal density for field emission has been carried out. In the extensively studied vapor−liquid−solid (VLS) method, the ZnO nanowire density can be tuned by controlling either the density of the Au catalyst nanoparticle or the thickness of the Au film.[5,6] For example, Wang et al.[6] demonstrated that the nanowire density decreases from 11.2×10^9 to 1.5×10^9 cm^{-2} when the thickness of the gold film increases from 1 to 8 nm. The best field emission performance from these nanowire films was obtained from nanowire arrays with densities between 6×10^9 and 8×10^9 cm^{-2}. Though the VLS method has good density control capability, the high-temperature (>900 °C) growth process is incompatible with the typical fabrication procedure of vacuum micro/nano electronic devices.[7]

Recent successes in the synthesis of ZnO nanowires by using the low-temperature solution-phase method provide an alternative way to develop ZnO nanowire-based field electron emission devices.[8,9] As compared to its high-temperature counterparts, the solution-phase method has merits of low temperature, no catalyst, low cost, ease of scale-up, and ease for pattern growth.[10] Very recently, the density controllable synthesis of ZnO nanowires by the solution-phase method has made some progress.[11,12] For example, Ma et al.[11] prepared the ZnO nanoparticles as the seed for nanowire growth by spin coating the zinc acetate colloid followed by thermal annealing (>300 °C). The density of the nanowires was adjusted by tuning the colloid concentration, spin coating time, annealing temperature, and annealing time. It was found that the density could be changed within 4 orders of magnitude, i.e., from 1.73×10^{10} to 1.3×10^6 cm^{-2}. Accordingly the diameter of nanowires increased from 72 nm to 2.2 μm. Alternatively, Song et al.[12] used ZnO film as the seed-layer prepared by sputtering. The density of the nanowires was tuned by adjusting the seed-layer thickness. When the seed-layer thickness increased from 200 to 950 nm, the density decreased within a narrow range, i.e., from 3.2×10^9 to 2×10^9 cm^{-2}. Meanwhile, the diameter increased from 50 to 80 nm. As compared to controlling the nanowire density by tuning the ZnO nanoparticle density,[11] tuning the nanowire density by changing the thickness of seed-layers has the advantages of a simple process and no need for a high-temperature thermal annealing process.

However, despite strong effort and interest, the development of a facile method for tuning the density in a wide range remains a challenge. Meanwhile, the mechanism responsible for the variation of nanowire density by changing the thickness of the seed-layer is not fully clear. More importantly, the effect of the change of the nanowire density on the field emission has not been investigated. It is known that the diameter and the height of the nanowires are varied in accord with the density. It is difficult to obtain both the optimal density and the large aspect ratio in one synthesis process by the solution-phase method. As stated at the beginning, the density, the diameter, and the height altogether can affect field emission properties of nanowire films. Thus, it is necessary to find an optimal combination of these three parameters to obtain the better field emission properties from the ZnO nanowire films prepared by using the solution-phase method. Herein, we present (i) results of wide-range density tuning (more than 5 orders of magnitude), (ii) an

* Corresponding author. N.X.: phone +86-20-84110916, fax +86-20-84037855, e-mail stsxns@mail.sysu.edu.cn. J.S.: phone +86-20-84113295, fax +86-20-84037855, e-mail shejc@mail.sysu.edu.cn.

10.1021/jp8015563 CCC: $40.75
Published on Web 07/10/2008

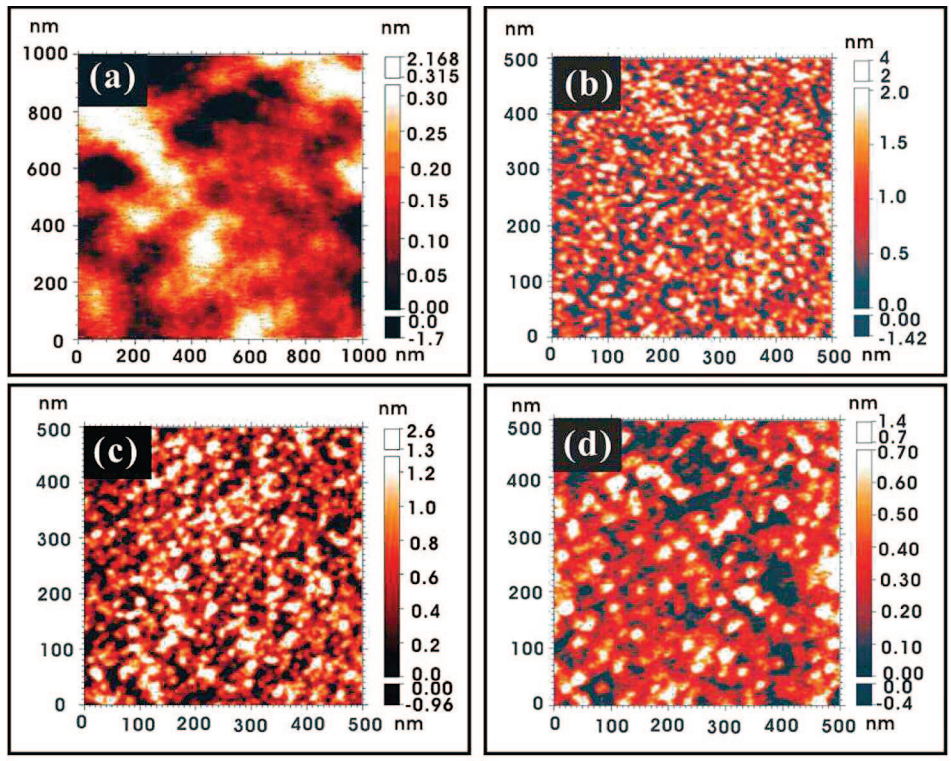

Figure 1. AFM images of the ZnO seed-layers with deposition times of 60 (b), 90 (c), and 210 s (d); panel a is that from a blank Si surface.

alternative model based on the seed-layer etching effect for understanding the density tuning mechanism, and (iii) a systematic field emission study to find an optimal combination of the three parameters.

2. Experimental Section

In the present work, efforts were first devoted to develop a technical procedure for tuning the density of the ZnO nanowires by changing the thickness of the ZnO seed-layer. We used 2 cm × 3 cm Si (100) substrate. The ultrathin ZnO films with different thickness were deposited on the different areas of the same substrate by employing the direct current sputtering technique. In the deposition, the target used is metallic zinc foil (99.99% in purity). Air was introduced as the sputtering gas. The film thickness was controlled by changing the deposition duration, i.e., 60 to 240 s with an increment of 30 s. Atomic force microscopy (AFM, Omicron) was used to characterize the morphology of the films. A surface profiler (Vecco Daktak 6M) was used to measure the film thickness. In addition, X-ray diffraction (XRD) measurements were carried out on the seed-layers for the purpose of characterizing the crystal size. However, due to the fact that the seed-layer is too thin, very week signals were obtained. The samples with ZnO films were then suspended in the nutrient solution for ZnO nanowire growth. The nutrient solution (180 mL) used was a mixture of 0.005 M zinc nitrate hexahydrate ($Zn(NO_3)_2 \cdot 6H_2O$) and 0.005 M hexamethylenetetramine (HMT, $C_6H_{12}N_4$). The growth was performed at 80 °C for 6 h. After growth, the samples were rinsed with deionized water and then dried with a nitrogen stream.

The as-synthesized products were characterized by high-resolution field-emission scanning electron microscopy (SEM: FEI Quanta 400F), high-resolution transmission electron microscopy (HRTEM: JEM-2010), energy dispersive X-ray (EDX) analysis, and X-ray diffraction (XRD). The field-emission studies were carried out in a chamber having a vacuum of ~1.0×10^{-7} Torr at room temperature. The sample was adhered to the surface of a high-conductivity copper disk and a metal anode with diameter of 1 mm was placed in front of and parallel to the sample surface. The separation between the anode and the cathode (nanowire sample) was kept to 200 μm.

3. Results and Discussion

3.1. Effects of the Seed-Layer Thickness on the Density, Diameter, and Height of Nanowires. AFM images of the ZnO seed-layers with different deposition times are showed in Figure 1. Figure 1a is the morphology of the Si substrate, showing a flat surface with very small variation in roughness. After 60 s of ZnO deposition, exiguous ZnO islands can be observed. The typical root-mean-square (rms) roughness is ~0.673 nm (Figure 1b). Further prolonging the deposition time, i.e., 90 (Figure 1c) and 210 s (Figure 1d), resulted in smoother surfaces (~0.431 and ~0.229 nm in rms roughness for 90 and 210 s deposition, respectively). These indicate that continuous films were formed. Profiler measurements indicated that the film thickness with deposition times of 90, 120, 150, 180, 210, and 240 are ~1.5, ~2.0, ~2.5, ~3.0, ~3.5, and ~4.0 nm, respectively. The error of the measured thickness is about 0.1 nm.

Panels a−e of Figure 2 are the typical SEM images of the nanowires obtained on the areas with the seed-layer thickness of 1.5, 2.0, 2.5, 3.0, and 3.5 nm, respectively. Panels h−l of Figure 2 are the corresponding tilt-view (80°) images of those in panels a−e. These figures show that the densities of the nanowires in different areas are distinctly different (see Table 1). The density of the nanowires is higher for the areas with thicker seed-layers. With a narrow change in seed-layer thickness (1.5−3.5 nm), the density can be changed in a wide range, i.e., from 6.8×10^4 to 2.6×10^{10} cm^{-2}. This tuning scale is wider than those of the previous works.[11,12] Moreover, the diameter and the height of the nanowires decreases as the seed-layer thickness increases, as shown in Table 1. Furthermore,

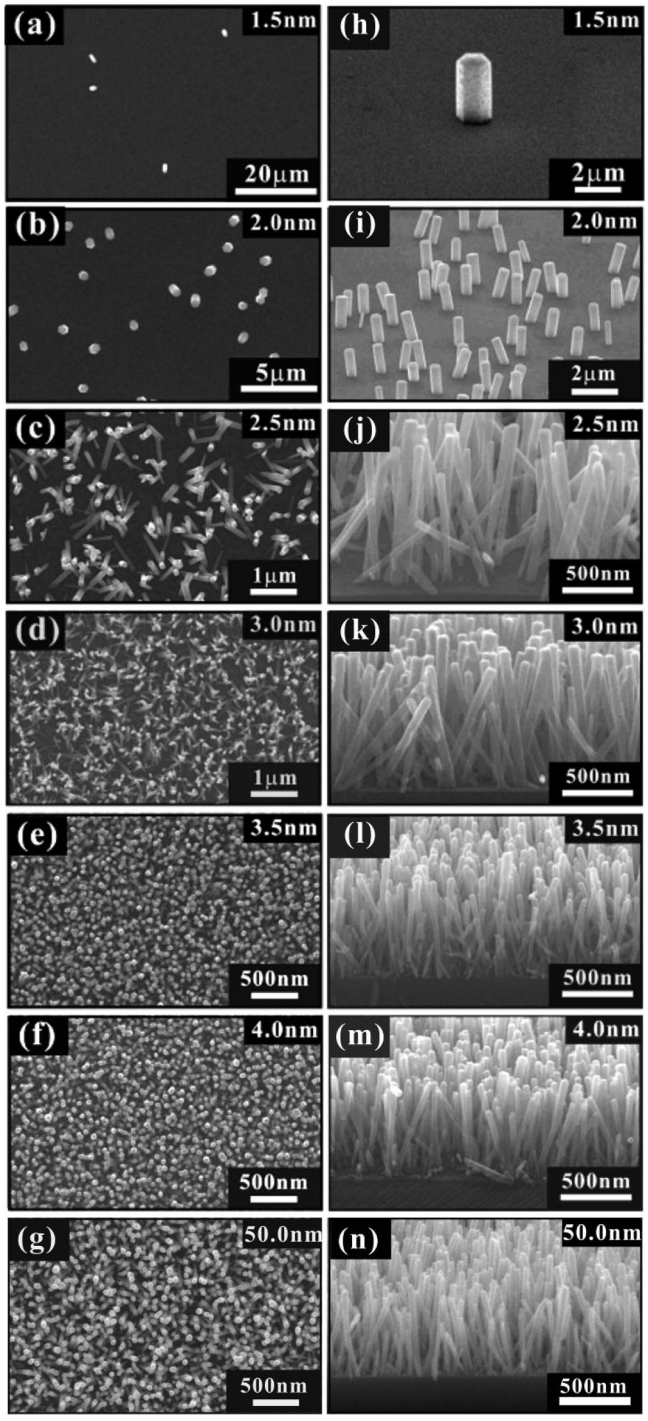

Figure 2. The typical SEM images of the nanowires: (a−g) the images of nanowires obtained from the areas with seed-layer thickness of 1.5, 2, 2.5, 3, 3.5, 4, and 50 nm, respectively; (h−n) the corresponding tilt-view (80°) image of that shown in panels a−g, respectively.

we have found the following two critical thicknesses: (i) If the seed-layer thickness is less than 1.5 nm, no nanowires were grown. (ii) If the seed-layer thickness is more than 3.5 nm, much less change in nanowire density and structural parameters was observed (see Figure 2e,f). For the purpose of supporting the second point, nanowires were grown on a seed-layer with a thickness of 50 nm. SEM investigation (Figure 2g,n) found that the density and the structural parameters of the nanowire are similar to those shown in panels e and l of Figure 2.

The nanowires were scraped from the Si substrate and collected by a carbon-coated Cu grid, then used for EDX and TEM characterizations. In the EDX spectra (Figure 3a), besides the Cu and C signals from the carbon-coated Cu TEM grid, only Zn and O were detected, demonstrating that the nanowires are pure zinc oxide. The HRTEM image and the corresponding selected-area electron diffraction pattern (Figure 3c) of an individual nanowire show that the lattice space between the adjacent lattice planes is ∼0.52 nm, confirming the [0001] growth direction for the single-crystal ZnO nanowires. Further characterization on the crystallographic properties of the nanowires was performed by XRD. The peaks (Figure 3d) for reflections from $(10\bar{1}0)$, (0002), $(10\bar{1}1)$, and $(10\bar{1}2)$ planes from the wurtzite ZnO crystal were observed. The strong (0002) diffraction peak at 34.62° indicates that the ZnO nanowires grow along the *c*-axis orientation, which is consistent with the HRTEM result.

Our finding on the effect of seed-layer thickness on the density and diameter of nanowires is different from the early result reported by Song et al.[11] They found that the diameter of the ZnO nanowires increased (from 50 to 80 nm) and the density decreased (from 3.2×10^9 to 2×10^9 cm^{-2}) as the seed-layer thickness increased (from 200 to 950 nm). We have found the opposite. Song et al. proposed that a larger crystal size form at thicker seed-layer might favor the growth of nanowires of bigger diameter, and the diameter increase further results in a decrease of nanowire density. This mechanism may be used to explain the reverse density changing behavior if the crystal size on our seed-layer is smaller on a thicker film. However, the model cannot explain why we observed the two critical thicknesses mentioned above. Although the mechanism for this reverse tendency on density changing is not fully understood yet, we proposed the following discussion.

In our experiments, the ultrathin seed-layers with different thickness were deposited on different areas of the same substrate. The nanowire growth was carried out in the same solution. Thus, the growth temperature (*T*), the content of Zn^+ and OH^- were the same. The only variable parameter is the thickness of the seed-layer. In the growth of the nanowires, the following chemical reactions take place,[13]

$$(CH_2)_6N_4 + 6H_2O = 6HCHO + 4NH_3 \quad (1)$$

$$NH_3 + H_2O \leftrightarrow NH_4^+ + OH^- \quad (2)$$

$$Zn^{2+} + 2OH^- \leftrightarrow Zn(OH)_2 \leftrightarrow ZnO_{(s)} + H_2O \quad (3)$$

Equations 1 and 2 illustrate the formation of OH^- needed for inducing the reactions in eq 3. The reaction given in reaction III is reversible.[14] In this reaction, the precursor Zn^{2+}reacts with OH^- to induce the growth of ZnO, also the ZnO seed can be etched away due to the equilibrium moving to the left. Namely, the growth and the etching of ZnO coexist. The reversibility may mainly depend on the diameter of the seed and the content of Zn and OH^-, but not on the thickness of the seed-layer. Due to this coexistence, the seed-layer can support the nanowires' growth only when its thickness exceeds a critical value (denoted as T_c, see Figure 4). Otherwise, it may be etched away before the nucleation process occurs. As illustrated in Figure 4a, for a very thin seed-layer (i.e., with 60 s deposition time), the exiguous ZnO seeds may be etched away before the nucleation occur. Thus, no nanowires will grow. Further prolonging the deposition time (i.e., 90 s), the seed-layer will become thicker. Due to fluctuation in the film thickness (see Figure 4b and the corresponding experimental evidence in Figure 1c), some sites (indicated with arrows) may be thick enough to sustain etching. Nucleations occur at these sites and thus the nanowires can grow. Further, it is reasonable to predict that more sites on a

TABLE 1: The Relationship between the Sputtering Times/Thickness of the ZnO Seed-Layers, the Nanowire's Geometric Parameters, and the Field Emission Properties

sputtering time	90 s	120 s	150 s	180 s	210 s
seed thickness (nm)	1.5	2.0	2.5	3.0	3.5
density (cm^{-2})	6.8×10^4	7.8×10^6	1.0×10^9	2.2×10^9	2.6×10^{10}
mean diameter 2r (nm)	1460	480	78	62	36
mean height h (μm)	2.6	1.20	1.03	0.92	0.62
E_{to}(V/μm)	no obtained	16.7	7.1	7.6	14.5
E_{thr}(V/μm)	no obtained	27.2	13.0	18.0	27.5
β	no obtained	291	862	850	398
d (μm)	36.8	3.1	0.24	0.15	0.030
s	1.000	0.997	0.417	0.315	0.106
β_{single} (aspect ratio, h/r)	3.56	5	26.4	29.6	34.4
β_{array} ($s(h/r)$)	3.56	4.985	11.009	9.324	3.646

thicker seed-layer can complete the nucleation process (Figure 4c). Consequently, denser ZnO nanowires can be obtained. However, when the seed-layer thickness is greater than the critical value T_c, i.e., 3.5 nm for the present case, the seed-layer is thick enough and the nucleation site may cover the entire surface (Figure 4d). Thus, high-density ZnO nanowires are formed. At this stage, due to the space-confining effect, further prolonging the deposition time will lead to much less effect on the changing of the nanowire density. According to this "etch and growth" mechanism, the etching effect is the main factor affecting the nucleation site density. However, in Song's work, the seed-layer thickness (i.e., >100 nm) is much thicker than the critical thickness (T_c = ~3.5 nm) we found. Thus, the etching effect is insignificant and the crystal size variation may be taken into the account. Therefore, a different tendency on density changing may be observed.

Furthermore, two possible mechanisms may explain the variation on nanowire's diameter and height. From the viewpoint

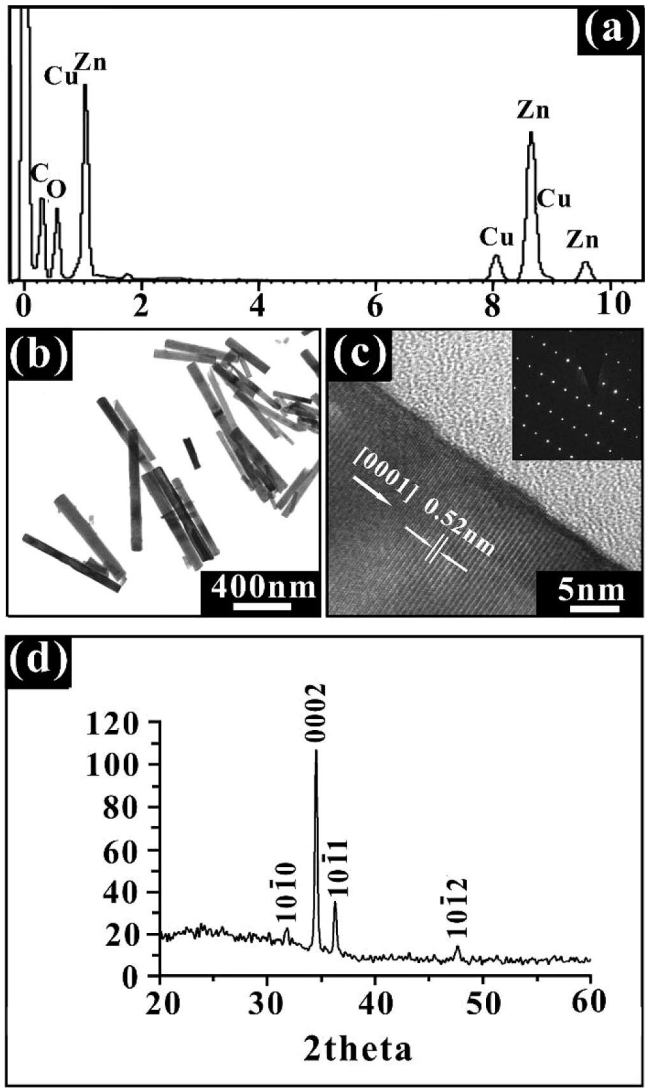

Figure 3. (a) The typical EDX spectra of the nanowires. (b−c) The typical TEM images of the nanowires. The inset is the corresponding SAED pattern. (d) A typical XRD spectra of the ZnO nanowires.

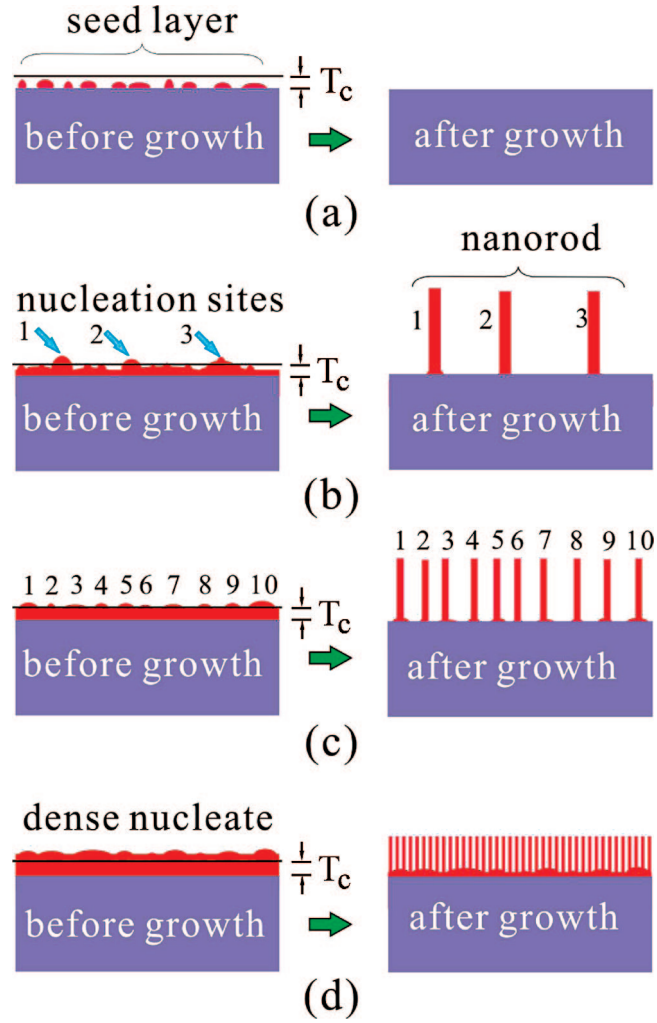

Figure 4. The schematic illustration showing how the seed-layer thickness affects the nanowire growth. T_c is the critical thickness value for the growth of ZnO nanowires. The numbers 1−10 indicate the sites with seed-layer thicker than T_c.

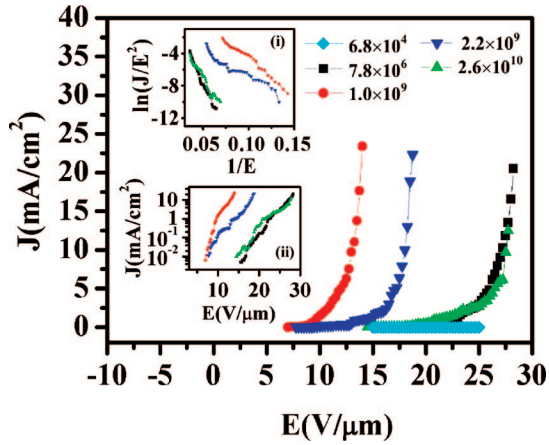

Figure 5. Field emission properties of the nanowires with different density. Inset i: the corresponding Flower−Nordheim (F−N) plots. Inset ii: The $J-E$ curve, which shows the current density with log scale.

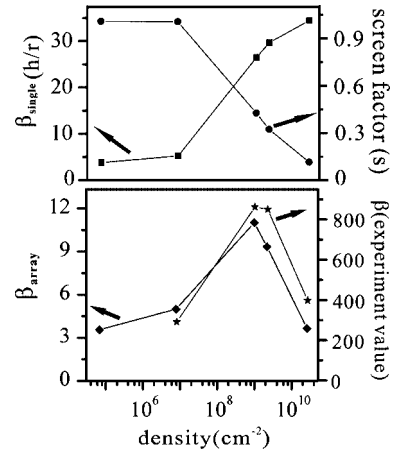

Figure 6. The change of the β_{single} (aspect ratio), screen effect factor (s), β_{array}, and experimental β value as the density variation.

of crystal growth, it is generally believed that the diameter of the ZnO nanowire is determined by the crystal size of the seed-layer.[12] Large crystal size often induces the growth of nanowires with larger diameter. Therefore, one of the possible mechanisms is the crystal size is smaller on a thicker seed-layer. However, crystal size may only affect the diameter, and it may have no significant effect on the height. Therefore, we propose another possible mechanism. We believe the consumption of Zn^{2+} may be higher at the area with dense nanowires. Thus, the local Zn^{2+} concentration may be lower. Therefore, the growth rate of the high-density nanowire is slower than that at the low-density area. This can explain why the dense nanowires are relatively shorter (see Table 1). Also, besides the fast consumption of Zn^{2+}, dense nanowires have narrow intervals, and thus the diffusion of Zn^{2+} is slower, which may lead to a slower growth rate of the nanowires' sidewalls. This second effect may be one of the reasons that can explain why the change in diameter is more sensitive than the change in height to the variation of density. With reference to Table 1, the nanowire with a density of 6.8×10^4 cm^{-2} is about 4 times higher and 40 times larger than those with a density of 2.6×10^{10} cm^{-2}. So the aspect ratio of the nanowire will increase as the density increases.

3.2. Effects on Field Emission. In the present experiment, the effects of the seed-layer on the density and the diameter and the height cannot be separated from each other. The effects of these three changes on the field emission properties have to be studied together with the purpose to find an optimal combination of density and aspect ratio. The emission current density was calculated by dividing the emission current by the anode area (0.785 mm^2). The turn-on field (E_{to}) and the threshold field (E_{thr}) are defined as the macroscopic fields required to produce a current density of 10 μA/cm^2 and 10 mA/cm^2, respectively. The typical field emission current density vs the applied field ($J-E$) curves from the nanowires with different density are shown in Figure 5. The corresponding Flower−Nordheim (F−N) plots were given as inset i. For the purpose of displaying the turn-on field clearly, the $J-E$ curve, which shows the emission current density with a log scale, was also given as inset ii. Table 1 listed the field emission characteristics. The nanowires with the lowest density (6×10^4 cm^{-2}) were found to have no detectable emission current even when a very high electric field (25 V/μm) was applied. The nanowires with relatively low density (7.8×10^6 cm^{-2}) and ultrahigh density (2.6×10^{10} cm^{-2}) both show poor field emission performance. The nanowires with a density of 1.0×10^9 cm^{-2} and the height of 1.03 μm and 39 nm in curvature radius were found to have the best field emission characteristics, with the lowest threshold and turn-on fields, i.e., 7.1 V/μm and 13 V/μm, respectively. The current density reached 23.4 mA/cm^2 at 14 V/μm. Though the field emission performance of the ZnO nanowires is not as good as those of carbon nanotube field emitters,[15] its unique low sysnthesis temperature makes it a candidate for vacuum micro/nano electronic device application.[16] According to the traditional F−N equation, the field enhancement factors (β) were calculated by using the slopes of the F−N plots and the work function of 5.3 eV.[1] The nanowires with medium density have larger β values, i.e., $\beta_1 = 862$ and $\beta_2 = 850$ for the nanowire with densities of 1.0×10^9 and 2.2×10^9 cm^{-2}, respectively. It is noted that this calculation has assumed the ZnO nanowires behave like metallic ones.

Since the nanowires are prepared on the same substrate, the sample-to-sample variation on materials properties such as conductivity and surface work function may be eliminated. Thus, it is reasonable to ascribe the difference in the field emission properties first to the variation on the nanowire density and their intrinsic aspect ratio. The latter directly affect the field enhancement: for a single emitter, its field enhancement factor can be described as $\beta_{single} \propto h/r$,[17] where h is the height and r is the radius of the emitter. But for nanowire arrays, field screening due to their close spacing may become significant, which can decrease the field enhancement at the tip of each nanowire dramatically. A screening factor (s) was introduced to characterize this screening effect: $s = \beta_{array}/\beta_{single}$.[18] The s value varies from 0 to 1. Smaller s means a stronger field screening effect. Bonard et al.[18] have proposed a model to estimate the screening effect in carbon nanotube (CNT) films. By electrostatic simulation, the s-value is mainly related to the height of the emitters (h) and the distance between two adjacent emitters (d). Typically, for the CNT emitters with height of $h_0 = 2$ μm, the s-value can be calculated from a function of $s = 1 - \exp(-1.1586d)$. For the CNTs with height h that is not equal to h_0, the relation becomes $s = 1 - \exp(-1.1586d(h_0/h))$.[18] Though the model is aimed at metallic CNTs emitters, we may use it to estimate the field screening effect of our ZnO samples, since at the present there is no specific model for ZnO nanowires. Using the h and d (listed in Table 1) obtained from the SEM measurements (Figure 2), the screen factors were calculated and listed in Table 1. Figure 6 shows how the aspect ratio, screen factor, β_{array}, and β-value obtained from F−N plots change as the density increases.

From Table 1, one may see that the diameter of the nanowires decreases faster than the height, as the density increases. This

has led to an increase of the aspect ratio and thus the β_{single} value. However, this increase was accompanied by the increase of the screening effect as the density increases. As a result, the really useful field enhancement value of the nanowires of the film, β_{array}, becomes smaller than the β_{single} value. From Figure 6, it is clearly shown that (i) the β_{array} has a relatively small value at a low density, i.e., 6.8×10^4 and 7.8×10^6 cm^{-2}, which is due to the small aspect ratio, (ii) the β_{array} still has a relatively small value at a high density of 2.6×10^{10} cm^{-2}, which is due to the large screen effect induced by the high density, and (iii) the β_{array} has a maximum value at a medium density of 1.0×10^9 cm^{-2}, which is due to the good combination of density and aspect ratio. The trend of β_{array} with the density is inconsistent with that of the β-value calculated from the F−N plots, as shown in Figure 6. On the other hand, however, the typical value of the β_{array} is more than an order of magnitude smaller than the typical β-value calculated from F−N plots. This means that there must exist some other mechanism responsible for the enhanced field emission. We expect that field-induced band-bending at the tip of a ZnO nanowire may be responsible. Much more needs to be done to examine this assumption.

From the above analysis, the nanowires with a medium density ($\sim 10^9$ cm^{-2}) and relative high aspect ration ($\sim$26) were found to have better field emission turn-on and threshold fields. This can partially be attributed to a good combination of density and aspect ratio. Further improvement may be possible if at a desirable density the aspect ratio may be increased by changing the height and diameter.

4. Conclusions

In summary, we investigated the effect of seed-layer thickness on the synthesis of ZnO nanowires and the consequence on their field emission characteristics. It is found that the density, diameter, and height of the ZnO nanowires are very sensitive to the thickness of the seed-layer within a very narrow range of seed-layer thickness from 1.5 to 3.5 nm. If the thickness is too small, no ZnO nanowires are formed, while when the thickness is larger than a certain value, e.g., 3.5 nm in the present study, the change in density will become less obvious. In the present study, when the thickness changes from 1.5 to 3.5 nm, the nanowire density has more than 5 orders of magnitude of increase, i.e., increased from 6.8×10^4 to 2.6×10^{10} cm^{-2}, while these changes are accompanied by a decrease in diameter, from 1460 to 36 nm, and a decrease in height, from 2.6 to 0.62 μm. The decrease in diameter is faster than that in height, and thus the aspect ratio increases by about an order of magnitude when the density increases. This increase in aspect ratio is not fully reflected in the enhancement of field emission because the increase in the density results in a field screening effect. These changes in aspect ratio and field screening effect have an obvious effect on field emission characteristics, represented by large changes in both the turn-on field and the threshold field: the former changes from 7.1 to 16.7 V/μm, and the latter from 13.0 to 27.5 V/μm. When the β_{array} is at its maximum, which takes into account a combination of the aspect ratio and the field screening effect, both turn-on and threshold fields are at their minimum. This demonstrates that optimal conditions can be found for field emission, under which ZnO nanowire films are prepared with the low-temperature solution-phase method. Further development of the control growth technique may lead to even better field emission characteristics of ZnO nanowires.

Acknowledgment. The authors gratefully acknowledge the financial support of the project from the National Basic Research Program of China (973 Program, Grant No. 2007CB935501), the National Natural Science Foundation of China (Grant Nos. U0634002, 60601019, and 60771055), the Science and Technology Ministry of China (Grant Nos. 2003CB314701 and 2007CB935501), the Education Ministry of China, the Science and Technology Department of Guangdong Province, the Education Department of Guangdong Province, and the Science and Technology Department of Guangzhou City. J.C.S. is also thankful for the support of the projects from the Natural Science Foundation of Guangdong Province (Grant No. 06300340) and Sun Yat-sen University.

References and Notes

(1) Lee, C. J.; Lee, T. J.; Lyu, S. C.; Zhang, Y.; Ruh, H.; Lee, H. J. *Appl. Phys. Lett.* **2002**, *81*, 19.
(2) Zhu, Y. W.; Zhang, H. Z.; Sun, X. C.; Feng, S. Q.; Xu, J.; Zhao, Q.; Xiang, B.; Wang, R. M.; Yu, D. P. *Appl. Phys. Lett.* **2003**, *83*, 144.
(3) Xu, C. X.; Sun, X. W. *Appl. Phys. Lett.* **2003**, *83*, 3806.
(4) Yang, Y. H.; Wang, B.; Xu, N. S.; Yang, G. W. *Appl. Phys. Lett.* **2006**, *89*, 043108.
(5) Jo, S. H.; Lao, J. Y.; Ren, Z. F.; Farrer, R. A.; Baldacchini, T.; Fourkas, J. T. *Appl. Phys. Lett.* **2003**, *83*, 4821.
(6) Wang, X. D.; Zhou, J.; Lao, C. S.; Song, J. H.; Xu, N. S.; Wang, Z. L. *Adv. Mater.* **2007**, *19*, 1627.
(7) Wang, Z. L. *Mater. Today* **2007**, *10*, 20.
(8) Vayssieres, L. *Adv. Mater.* **2003**, *15*, 464.
(9) Greene, L. E.; Law, M.; Goldberger, J.; Kim, F.; Johnson, J. C.; Zhang, Y. F.; Saykally, R. J.; Yang, P. D. *Angew. Chem., Int. Ed.* **2003**, *42*, 3031.
(10) Kang, B. S.; Pearton, S. J.; Ren, F. *Appl. Phys. Lett.* **2007**, *90*, 083104.
(11) Ma, T.; Guo, M.; Zhang, M.; Zhang, Y. J.; Wang, X. D. *Nanotechnology* **2007**, *18*, 035605.
(12) Song, J.; Lim, S. *J. Phys. Chem. C* **2007**, *111*, 596.
(13) Sun, Y.; Riley, D. J.; Ashfold, M. N. R. *J. Phys. Chem. B* **2006**, *110*, 15186.
(14) Wei, A.; Sun, X. W.; Xu, C. X.; Dong, Z. L.; Yang, Y.; Tan, S. T.; Huang, W. *Nanotechnology* **2006**, *17*, 1740.
(15) Bonard, J. M.; Salvetat, J. P.; Stöckli, T.; Heer, W. A. D.; Forró, L.; Châtelain, A. *Appl. Phys. Lett.* **1998**, *73*, 918.
(16) Lee, C. Y.; Tseng, T. Y.; Li, S. Y.; Lin, P. *Nanotechnology* **2006**, *17*, 83.
(17) Xu, N. S.; Huq, S. E. *Mater. Sci. Eng., R* **2005**, *48*, 47.
(18) Bonard, J. M.; Weiss, N.; Kind, H.; Stöckli, T.; Forró, L.; Kern, K.; Châtelain, A. *Adv. Mater.* **2001**, *13*, 184.

JP8015563